Projectile breakup dynamics for ^{6}Li + ^{59}Co: kinematical analysis of α-d coincidences

F. A. Souza[1a], N. Carlin[1], C. Beck[2], N. Keeley[3], A. Diaz-Torres[4], R. Liguori Neto[1], C. Siqueira-Mello[1], M. M. de Moura[1], M. G. Munhoz[1], R. A. N. Oliveira[1], M. G. Del Santo[1], A. A. P. Suaide[1], E. M. Szanto[1], and A. Szanto de Toledo[1]

[1] Instituto de Física - Universidade de São Paulo, Departamento de Física Nuclear, C.P. 66318, 05315-970, São Paulo-SP, Brazil

[2] Institut Pluridisciplinaire Hubert Curien, UMR 7178, CNRS-IN2P3 et Université Louis Pasteur, Boîte Postale 28, F-67037 Strasbourg, Cedex 2, France

[3] Department of Nuclear Reactions, The Andrzej Sołtan Institute for Nuclear Studies, ul. Hoża 69, 00-681 Warsaw, Poland.

[4] Department of Physics, Faculty of Engineering and Physical Sciences, University of Surrey, Guildford, GU2 7XH, UK

Abstract. A study of the kinematics of the α-d coincidences in the ^{6}Li + ^{59}Co system at a bombarding energy of $E_{\mathrm{lab}} = 29.6$ MeV is presented. With exclusive measurements performed over different angular intervals it is possible to identify the respective contributions of the sequential and direct projectile breakup components. The angular distributions of both breakup components are fairly well described by the Continuum-Discretized Coupled-Channels framework (CDCC). Furthermore, a careful analysis of these processes using a semiclassical approach provides information on both their lifetime and their distance of occurrence with respect to the target. Breakup to the low-lying (near-threshold) continuum is delayed, and happens at large internuclear distances. This suggests that the influence of the projectile breakup on the complete fusion process can be related essentially to direct breakup to the ^{6}Li high-lying continuum spectrum.

arXiv:0909.5556v2 [nucl-ex] 4 Mar 2010

1 Introduction

The breakup process in reactions induced by weakly bound nuclei (such as ^{6}Li on ^{28}Si [1], ^{59}Co [2,3], ^{64}Zn [4], ^{208}Pb [5], ^{209}Bi [6]; ^{7}Li+^{65}Cu [7] and ^{9}Be+^{244}Sm [8]) and its influence on the fusion cross section [9,10,11,12,13,14,15,16, 17,18,19,20,21,22] has been the subject of several experimental and theoretical investigations in recent years. In inclusive experiments, the light particle spectra measured in 'singles' mode display significant contributions from reaction mechanisms other than projectile breakup [5,23, 24]. This was also shown very recently for the well studied ^{6}Li + ^{59}Co system [2,3]. The consideration of either total fusion cross sections or complete fusion (CF) cross sections has proved to be important for a better understanding of the competition between the different mechanisms and their respective influence on the fusion process. The contributions of sequential projectile breakup (SBU) and direct projectile breakup (DBU) are both significant and it is necessary to determine which process influences CF most. In this case, a study of the breakup dynamics could provide decisive information.

The direct breakup DBU seems to be the main cause of the above-barrier CF suppression in the ^{9}Be + ^{208}Pb system, as shown in [25] through sub-barrier measurements of the breakup probability as a function of the distance of closest approach. This is a key ingredient for a novel classical trajectory model with stochastic breakup [26] which quantitatively relates the breakup process to the ICF and CF cross sections.

^a e-mail: fsouza@dfn.if.usp.br

In this work, we present the results of α-d coincidence measurements (non-capture breakup events) for the ^{6}Li + ^{59}Co system at a bombarding energy of $E_{lab} = 29.6$ MeV, about twice the energy of the Coulomb barrier. The same analysis can be applied and similar conclusions may be drawn for the other lower energies studied in our previous work [2]. However, we have chosen to present the results for the highest available energy since it exhibits the largest measured exclusive cross sections, i.e. the statistics for binary (projectile breakup and transfer) events are high enough to allow a very careful semiclassical analysis. By using a simple 3-body kinematics analysis we demonstrate that the incomplete fusion (ICF) and/or transfer (TR) processes on the one hand, and the projectile breakup components (SBU and DBU) on the other, are associated with quite different angular intervals. In ref. [2] we presented results from singles measurements which show that there is a significant contribution of the ICF/TR processes, i.e. no distinction between the contributions of ICF and TR was possible. In order to gather informations on this important subject, in this work we also present the results of an investigation of the breakup dynamics, by means of calculations related to semiclassical considerations [27] involving barrier tunnelling, lifetimes and distances of closest approach for the Coulomb trajectories of the projectile and outgoing fragments. Through this analysis with exclusive measurements we intend to study the influence of the breakup on CF by determining the distance of occurrence from the target of the SBU and DBU components.

2 Experimental Setup

The experiment was performed at the University of São Paulo Pelletron Laboratory, using the 8 UD Tandem accelerator. The 30 MeV ^{6}Li beam was provided by a SNICS ion source and bombarded a 2.2 mg/cm^2 ^{59}Co target. It is interesting to note that the energy spectra were not at all affected by the relatively large thickness of the target, as shown by Fig. 1, for example. After correction for energy loss in the target, the effective bombarding energy was $E_{\text{lab}} = 29.6$ MeV ($E_{\text{cm}} = 26.9$ MeV) more than twice the energy ($E_{\text{cm}} \approx 12$ MeV) corresponding to the Coulomb barrier. The beam current on target was about 10 nA. We used 11 triple telescopes [28] for the detection and identification of the light particles, positioned on both sides of the beam axis with 10° spacing, covering angular intervals from $-45°$ to $-15°$ and 15° to 75°. The telescopes consisted of an ion chamber with a 150 μg/cm^2 aluminized polypropylene entrance window, a 150 μm thick Si surface barrier detector and a CsI detector with PIN diode readout. The ion chamber was operated with 20 torr of isobutane.
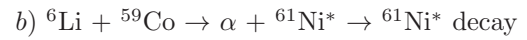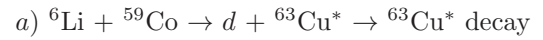
Additional details of the experimental setup and light charged particle analysis can be found elsewhere [2,28].

3 Results and discussion

In a previous publication [2], we investigated the kinematics of the inclusive α and d energy spectra. After subtraction of the estimated compound nucleus contributions, broad bumps with significant yields remained in both the α and d spectra. The behaviour of the energy centroids of these bumps as a function of the detection angle was found to be consistent with dominant contributions from incomplete fusion and/or transfer components i.e.: α-incomplete fusion (α-ICF)/α-transfer (α-TR) for the d spectra and d-incomplete fusion (d-ICF)/d-transfer (d-TR) for the α spectra.

These processes are represented, respectively, as follows:

a) ^{6}Li + ^{59}Co $\rightarrow d$ + ^{63}Cu* $\rightarrow$ ^{63}Cu* decay

b) ^{6}Li + ^{59}Co $\rightarrow \alpha$ + ^{61}Ni* $\rightarrow$ ^{61}Ni* decay

The corresponding excitation energies (associated with the energy centroids of the bumps) were 24.6 MeV and 22.5 MeV for the ^{61}Ni and ^{63}Cu nuclei, respectively.

In fig. 1 typical two-dimensional α-d coincidence spectra are displayed. The large target thickness did not affect the good energy resolution achieved, shown, for example, by the narrow peaks in the deuteron spectra of Fig.1.(b). For angular differences within the ^{6}Li breakup cone corresponding to the (2.186 MeV, 3$^+$) first resonant state we observed two peaks from the two possible kinematical solutions of the SBU. We also observed a broad structure between the two sharp peaks. Alpha-d decay of the second excited state (3.562 MeV, 0$^+$) of ^{6}Li is forbidden due to parity considerations and no peak due to the third excited state (4.312 MeV, 2$^+$) was observed. No evidence of decays from higher-lying resonant states was seen. For angular differences larger than the SBU cone, we observed only
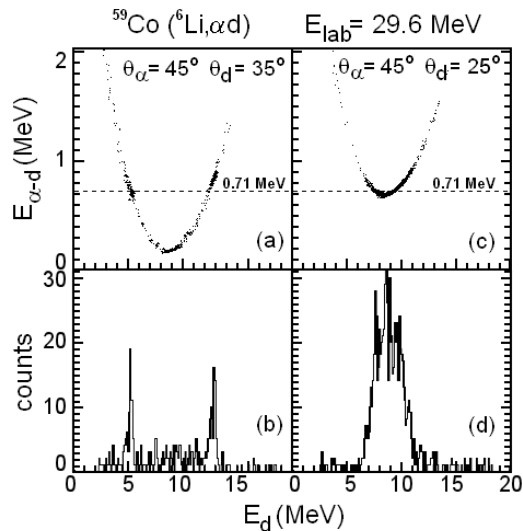
Fig. 1. a) The α-d relative energy $E_{\alpha d}$ as a function of the deuteron energy for $\theta_\alpha = 45°$ and $\theta_d = 35°$. b) The corresponding projection on the deuteron energy axis. c) and d) The same for $\theta_\alpha = 45°$ and $\theta_d = 25°$. The dashed lines correspond to 3-body kinematics calculations assuming α-d decays from the first resonant (2.186 MeV, 3^+) state of ^{6}Li.

broad structures. These broad structures could be associated with either the decay of nuclei produced in ICF/TR (incomplete fusion and/or transfer) or ^{6}Li DBU to the continuum. For ^{6}Li + ^{198}Pt, Shrivastava et al. [29] have measured cross sections for d capture (i.e. corresponding to the scenario previously defined as b) with d-ICF) that are much larger than TR cross sections. It is also interesting to note that these non-resonant contributions were assumed to arise exclusively from DBU in the case of the ^{6}Li + ^{209}Bi reaction [6] at E_{lab} = 36 MeV and 40 MeV whereas ICF yields were found to represent a large fraction of the total reaction cross section in this energy range [12].

3.1 Kinematics of the α-d coincidences

In order to identify the contributions of the different mechanisms included in the broad structures, we performed a 3-body kinematics [30] analysis of the α-d coincidence events. We present a study of the α and d energies as a function of angle and, as in previous work, we investigate the behaviour of the energy centroids of the broad structures. For the case of fixed α-particle angle, if d-ICF/TR is dominant the α-particle energy should be constant, independent of the d emission angle. This energy should be consistent with the excitation energy of the intermediate ^{61}Ni nucleus. Similar behaviour would be expected for fixed d angle in the case of dominant α-ICF/TR; the d energy should be constant as a function of the α-particle emission angle and consistent with the excitation energy of the ^{63}Cu intermediate nucleus. On the other hand, as shown in [31,32], if ^{6}Li direct breakup is dominant, the centroid of the broad structure would approximately correspond to the minimum allowed α-d relative energy for each angular pair (see fig. 1).

In fig. 2 we plot the d energy E_d as a function of θ_α for $\theta_d = 35°$. In this case, if α-ICF/TR is dominant, the d energy E_d should be constant, consistent with the 22.5 MeV excitation energy of the ^{63}Cu intermediate nucleus (dotted line). This behaviour would be more evident for angles near the ^{63}Cu recoil direction, for which we expect the maximum of cross section for the α-particle decay. This is indeed observed for angles near the recoiling ^{63}Cu. For other negative angles we observe instead a trend consistent with a 24.6 MeV excitation energy for the ^{61}Ni compos-
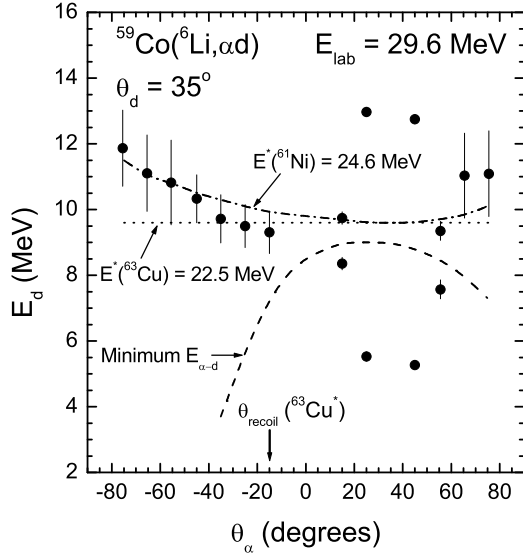
Fig. 2. Experimental values for the deuteron energy as a function of the α-particle detection angle. The 3-body kinematics predictions for ICF/TR and the minimum relative energy, $E_{\alpha d}$, for ^{6}Li breakup are also shown.

ite system (dot-dashed line). This suggests the dominance of the d-ICF/TR process. Therefore, both α-ICF/TR and d-ICF/TR contributions can be, in principle, mixed together. The behaviour of the minimum allowed α-d relative energy for ^{6}Li breakup is also shown in fig. 2 (dashed line). The observed trend suggests that the ^{6}Li DBU dominates in the case of angular pairs for which the broad structure is observed with $\Delta\theta_{\alpha d} = 10°$ and $20°$. For these angular pairs (i.e. for θ_α angle values ranging between $10°$ and $50°$) the experimental points shown in fig. 2 correspond to the energies of the SBU peaks clearly visible in fig. 1(b) and extrapolated in fig. 1(d).

3.2 Breakup dynamics

In order to gain insight into the dynamics of the SBU and DBU processes, we use a semiclassical approximation, following the procedure previously adopted in [33]. This hypothesis is valid as long as the Sommerfeld parameter η is large ($\eta \sim 6$). High partial waves of the projectile-target relative motion dominate the non-capture breakup process, so the effect of the nuclear field on the projectile trajectory is very small. We can then assume that the projectile travels through the target nuclear field following a Coulomb trajectory. This statement is also valid for the breakup fragments, as long as the relative energies are not too high.

The relation between the angle of emission and the distance of closest approach is:

$$R_{min} = \frac{Z_p Z_T e^2}{2E} \left[1 + \frac{1}{\sin(\theta/2)} \right] \quad (1)$$

where Z_p and Z_T are the projectile and target charge numbers, E is the centre-of-mass energy and θ is the scattering angle.

In order to obtain information on the distances of closest approach related to the occurrence of SBU and DBU, we define a quantity f which may be considered as the relative probability for the production of particles for a given process at a given distance of closest approach. The quantity f may be defined as follows:

$$f = \frac{1}{R_{min}} \frac{d\sigma}{dR_{min}}$$
$$= -\frac{1}{R_{min}} \frac{16\pi E}{Z_p Z_T e^2} \sin(\theta/2) \frac{d\sigma}{d\Omega} \quad (2)$$

Here, $d\sigma/d\Omega$ is the differential cross section in the centre-of-mass rest frame for the process under consideration.

Figure 3 depicts the experimental angular distribution for the SBU process analyzed in ref. [2], as well as for the DBU. The angular distribution for the DBU is shown for ^{6}Li continuum excitation energies summed between E* = 1.66 MeV and E* = 2.10 MeV. In the semiclassical calculations, we adopted the most probable value of the excitation energy observed experimentally in this range, which is E* = 1.7 MeV. The dotted and dashed lines correspond to the SBU and DBU CDCC calculations, similar to those of [20], respectively. The $\alpha + d$ binning scheme was appropriately altered to accord exactly with the measured continuum excitation energy ranges. It should be noted that the calculated elastic scattering and the SBU cross sections are unaffected by the change in continuum binning scheme. The DBU CDCC result presents a fair agreement with the experimental DBU angular distribution at forward angles and a similar shape at backward angles, although a small difference in the magnitudes is observed. In table 1 we present the experimental ^{6}Li SBU cross section for the first resonant state (2.186 MeV, 3$^+$) [2] and experimental DBU cross sections for the three excitation energy intervals (ΔE^*) we observed, together with their corresponding CDCC predictions. The CDCC cross sections are in agreement with the experimental ones within the uncertainties (that are relatively large for the E^* range from 2.20 MeV to 2.40 MeV, as shown in the following) except for the E^* range from 3.10 MeV to 3.25 MeV which has a smaller cross section. In particular, for the DBU cross section corresponding to the E^* range from 2.20 MeV to 2.40 MeV, we have the situation as shown in fig. 1(c) and
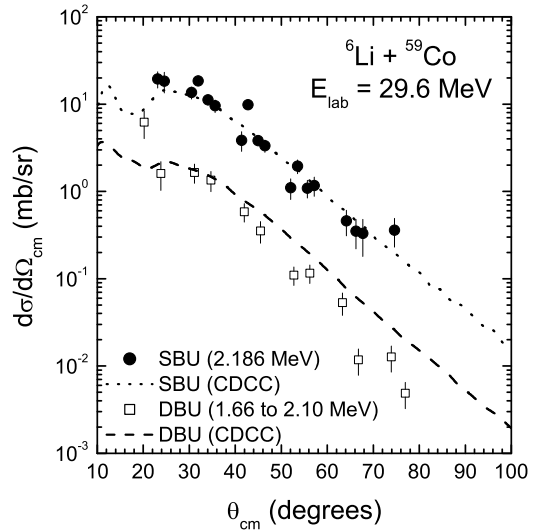

Fig. 3. Experimental angular distributions for the projectile sequential breakup (full circles) and direct breakup (open squares) processes, respectively. The dotted curve (CDCC calculation [20] for SBU) and dashed curve (CDCC calculation for DBU), as described in the text, are used for the semi-classical calculations of lifetimes and distance of occurrence discussed in fig. 4 and fig. 6.

fig. 1(d). In this case, the SBU is observed in the kinematical limit of the SBU cone, making the distinction between SBU and DBU more difficult. In order to overcome this problem, we adopted the procedure of calculating the cross section and subtracting the corresponding value of the SBU already determined in previous work [2] for the situation depicted in fig. 1(b), where there is no problem with the distinction between SBU and DBU. The clear separation of two sharp peaks, as well as their widths, in fig. 1(b) indicates that the broad structure observed in fig. 1(d) can not be related to effects of energy loss due to the target thickness.
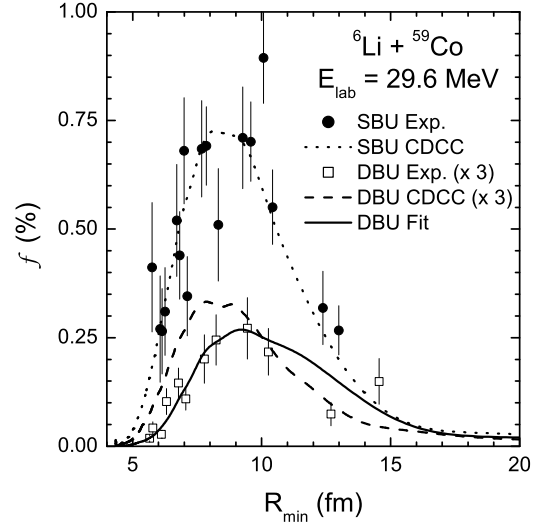
Table 1. Experimental SBU and DBU cross sections and CDCC predictions.

	ΔE^* (MeV)	σ_{Exp} (mb)	σ_{CDCC} (mb)
SBU [2]	2.186	20.6 ± 4.0	22.1
	1.66 - 2.10	3.04 ± 0.41	2.9
DBU	2.20 - 2.40	6.8 ± 4.2	3.5
	3.10 - 3.25	4.45 ± 0.94	2.3

Fig. 4. Function f representing the relative probability for production of particles of a given process at a given distance of closest approach, as a function of $R_{\min}$ for the projectile breakup processes SBU and DBU.

The curves presented in fig. 3 were used for the calculation of the f functions shown in fig. 4 as a function of $R_{\min}$ for the SBU and DBU processes. In particular, a fit to the experimental data represented by the solid curve was used for DBU. From the three curves in fig. 4, the quantity $R_{\min}^{\mathrm{MP}}$, the most probable value for $R_{\min}$ for the process of interest, is obtained.

The dip in the angular distributions is probably due to the effect of nuclear-Coulomb interference at forward angles ($\sim 20°$). This confirms that, as the incident energy is fairly high with respect to the Coulomb barrier, the nuclear effects persist to quite forward angles. In fig. 4, this interference effect is associated with a large $R_{\min}$ ($\gtrsim 15$ fm). If we took into account the nuclear interaction, essentially the tail of the f distribution would be affected. Therefore, we expect that the value of $R_{\min}^{\mathrm{MP}}$, and consequently the conclusions regarding the breakup distances of occurrence will not change.

In this work we also obtained insight into the lifetimes and distance of occurrence from the target for the SBU and DBU processes. In particular, for SBU we observed

that the main contribution is due to the ^{6}Li 3^+ state with $E^* = 2.186$ MeV. For the DBU, the fragments are no longer bound by the nuclear potential, but are still under the influence of the Coulomb barrier between the α-particle and the d. This means that at least for the smaller relative energies, the DBU is a delayed process, as is the SBU. A schematic representation of nuclear and Coulomb potentials is shown in fig. 5 (adapted from ref. [27]) as a function of the separation distance r between the α-particle and the d. The height of the Coulomb barrier $V_{\mathrm{B}} = 0.576$ MeV was obtained using $R_{\alpha d} = 5.0$ fm and the breakup threshold is defined at $E_{\alpha d} = 0$.

In order to estimate the DBU lifetime due to barrier tunnelling, we adopt the model of [27], where it was assumed that, as in the theory of α decay, the decay rate of
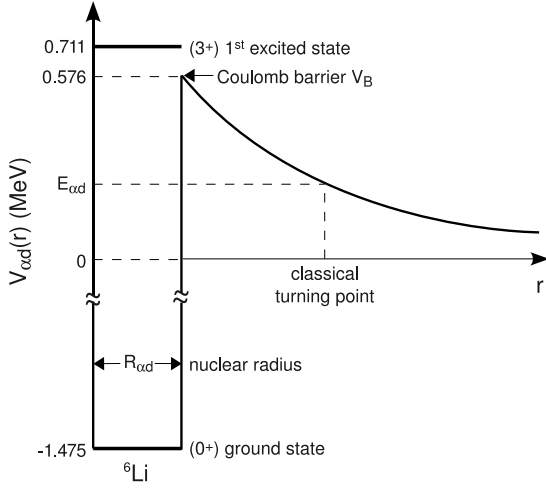
Fig. 5. Schematic representation of nuclear and Coulomb potentials as a function of the separation distance r between the α-particle and the d (adapted from ref. [27]).

the unbound system can be written as:

$$\Lambda_l = \omega_l P_l \tag{3}$$

where ω_l is the barrier bouncing frequency, and P_l is the barrier transmission probability. Considering that we are dealing with relatively low α-d relative energies, only the s-wave case for which $l = 0$ will be considered, for simplicity. In this situation, the bouncing frequency can be estimated as being $\omega_0 = v_{\alpha d}/2R$, where $v_{\alpha d}$ is the α-d relative velocity and R, the nuclear radius. The barrier transmission probability, according to the WKB approximation, is given by:

$$P_0 \approx \sqrt{\frac{V_B}{E_{\alpha d}}}\exp\left\{-4\eta\left[\frac{\pi}{2} - \arcsin\sqrt{\frac{E_{\alpha d}}{V_B}}\right.\right.$$
$$\left.\left. -\sqrt{\frac{E_{\alpha d}}{V_B}\left(1 - \frac{E_{\alpha d}}{V_B}\right)}\right]\right\} \tag{4}$$

where $\eta = Z_\alpha Z_d e^2/\hbar v_{\alpha d}$ is the Sommerfeld parameter and $V_B = Z_\alpha Z_d e^2/R_{\alpha d}$ is the height of Coulomb Barrier. The lifetime can then be determined as $\tau = 1/\Lambda$.

Following Coulomb excitation first order perturbation theory [34] and using the time of Coulomb excitation as the reference for measuring the lifetime [27], one can estimate the distance between projectile and target when DBU occurs. According to [34,27], in the focal system of the hyperbolic orbit, the distance between projectile and target can be written as:

$$r = a[\varepsilon \cosh(s) + 1]. \tag{5}$$

Here, a is half the distance of closest approach for a head-on collision, ε is the eccentricity parameter, given by $\varepsilon = 1/\sin(\theta^{MP}/2)$, with θ^{MP} being the scattering angle associated with $R_{\min}^{MP}$. The parameter s [34,27] is related to the time t by:

$$t = \frac{a}{v}[\varepsilon \sinh(s) + s], \tag{6}$$

where v is the initial relative velocity of projectile and target.

As described above, from eq. 3 and $l = 0$, we can determine the lifetime $\tau_{DBU} = 1/\Lambda_{DBU}$ for the DBU states near threshold. In fig. 6 we present the plot of τ_{DBU} ($E_{lab} = 29.6$ MeV) as a function of $E_{\alpha d}$. Besides the ^{6}Li continuum at excitation energy $E^* = 1.7$ MeV shown in fig. 3, contributions from $E^* = 2.3$ MeV and 3.2 MeV were also observed. Through eq. 6, and using the ^{6}Li excitation energies with the corresponding values of τ_{DBU} (in this case $t = \tau_{DBU}$), the values of s can be determined and used in eq. 5 to obtain r_{DBU}. The values of r_{DBU} can be compared to those obtained for SBU from the ^{6}Li 3^+ state with $E^* = 2.186$ MeV, and knowing that the SBU lifetime is $\tau_{SBU} = 2.73 \times 10^{-20}$ s, corresponding to
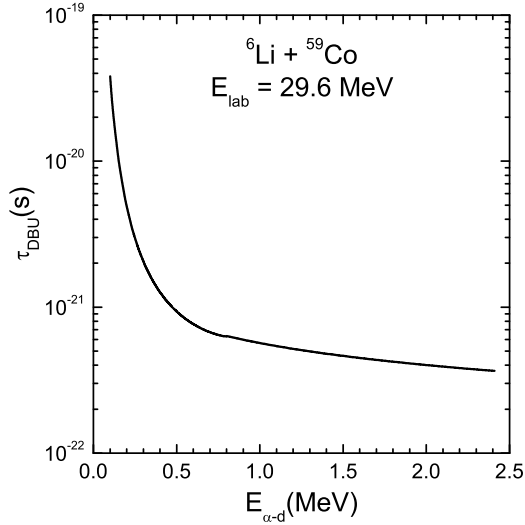
Fig. 6. Calculated lifetime of the DBU continuum states as a function of the relative energy $E_{\alpha d}$ from which the corresponding distances of occurrence can be deduced in table 2.

Table 2. Lifetimes, average distance of closest approach and distance of occurrence from the target for the projectile breakup components SBU and DBU.

	E^* (MeV)	τ (s)	R_{min}^{MP} (fm)	r (fm)
SBU	2.18	2.7×10^{-20}	8.5 ± 0.4	831.0 ± 1.3
DBU	1.7	4.9×10^{-21}	8.3 ± 0.4^a	143.1 ± 1.5
	1.7	4.9×10^{-21}	9.2 ± 0.5^b	147.2 ± 1.7
	2.3	6.3×10^{-22}	9.1 ± 0.7	19.8 ± 0.8
	3.2	4.4×10^{-22}	8.1 ± 1.2	14.3 ± 1.8

^{a} and ^{b}: from dashed and solid lines in fig. 4, respectively.

$\Gamma_{SBU} = (0.024 \pm 0.002)$ MeV [35]. The results described above are summarized in table 2. Note that the values of r obtained through the two functions f for DBU in fig. 4 are very similar.

Table 2 shows that for all the processes we considered the values of R_{min}^{MP} are very similar. However, the distances

of occurrence are very distinct for the SBU and DBU. Due to the long lifetime of the resonant ^{6}Li first excited state, sequential projectile breakup occurs very far from the target. On the other hand, for DBU the shorter lifetimes of the continuum 'states' cause the breakup process to occur at shorter distances from the target, although there are different distances for different excitation energies in the continuum.

The results obtained in this work are related to the non-capture breakup processes as defined in ref. [9]. However, they can also be extended to the case in which only one of the cluster constituents of the projectile is captured by the target after projectile breakup. As observed in ref. [2], from the investigation of the inclusive data, the ICF/TR component has been found to have the largest cross section, and therefore has the major influence on the CF cross section. This conclusion appears to be also valid for a heavy target reaction such as ^{6}Li + ^{209}Bi [6] or ^{6}Li + ^{198}Pt [29]. Our results as well as refs. [6,29] may indicate that the flux diverted from CF to ICF would arise essentially from DBU processes via high-lying continuum (non-resonant) states of ^{6}Li; this is due to the fact that both the SBU mechanism and the low-lying DBU processes from low-lying resonant ^{6}Li states occur at large internuclear distances. The importance of ICF (or the so-called fusion suppression [12,13,25]) in reactions induced by weakly-bound projectiles is still open. It has been shown recently [36] that for a particular projectile (^{6}Li, ^{7}Li or ^{9}Be, for instance), ICF cross sections increase with the charge of the target. But, similarly, fusion sup-

pression (i.e. ICF) increases with the breakup threshold of the projectile. Work is still in progress to study ICF processes for ^{6}Li + ^{59}Co within the 3-dimensional classical trajectory model of Diaz-Torres and collaborators [26].

4 Summary

In a previous study of the reaction mechanisms in the ^{6}Li + ^{59}Co reaction at four different bombarding energies, namely, E_{lab} = 17.4 MeV, 21.5 MeV, 25.5 MeV and 29.6 MeV [2], we mainly showed results of the sequential breakup SBU. In the present work we investigated the kinematics for α-d coincidences registered for the ^{6}Li + ^{59}Co reaction at E_{lab} = 29.6 MeV, approximately twice the energy of the Coulomb barrier. The analysis of the present exclusive α-d (energy and angular correlations) data along with 3-body kinematics calculations allowed us to observe that the ICF/TR and the SBU/DBU processes are associated with distinct angular regions. The measured breakup (SBU and DBU) cross sections, both consistent with Continuum-Discretized Coupled-Channels (CDCC) calculations, are found to be much larger than for the study with the ^{28}Si target [1], as might be expected from the greater importance of Coulomb breakup for the ^{59}Co target. The same conclusions can be drawn for the three other lower bombarding energies. In order to complement the results of singles measurements presented in ref. [2], a semiclassical approach, known to be valid in this energy range, was used to estimate the lifetime and distance of occurrence with respect to the ^{59}Co target for SBU and DBU. The results indicate that projectile breakup to the low-lying (near-threshold) continuum is delayed, and occurs at large internuclear distances. To conclude, for ^{6}Li + ^{59}Co the influence of breakup on the CF process is essentially due to DBU to the ^{6}Li high-lying continuum spectrum, i.e., the flux diverted from CF to ICF is due to DBU states.

References

1. A. Pakou *et al.*, Phys. Lett. B **633**, 691 (2006).

2. F. A. Souza *et al.*, Nucl. Phys. A **821**, 36 (2009);arXiv:**0811.4556**(2009).

3. F. A. Souza *et al.*, Nucl. Phys. A **834**, 420 (2010); arXiv: **arXiv:0910.0342** [nucl-ex] (2009).

4. P. R. S. Gomes *et al.*, Phys. Rev. C **71**, 017601 (2005).

5. C. Signorini *et al.*, Phys. Rev. C **67**, 044607 (2003).

6. S. Santra *et al.*, Phys. Lett. B **677**, 139 (2009).

7. A. Shrivastava *et al.*, Phys Lett. B **633**, 463 (2006).

8. P. R. S. Gomes *et al.*, Phys. Lett. B **634**, 356 (2006).

9. L. F. Canto, P. R. S. Gomes, R. Donangelo and M. S. Hussein, Phys. Rep. **424**, 1 (2006).

10. N. Keeley, R. Raabe, N. Alamanos, and J. L. Sida, Prog. Part. Nucl. Phys. **59**, 579 (2007); arXiv: **0702038** [nucl-th] (2007) and references therein.

11. L. F. Canto, P. R. S. Gomes, J. Lubian, L. C. Chamon, E. Crema, Nucl. Phys. A **821**, 51 (2009).

12. M. Dasgupta *et al.*, Phys. Rev. C **70**, 024606 (2004).

13. M. Dasgupta *et al.*, Phys. Rev. Lett. **82**, 1395 (1999); arXiv:**nucl-ex/9901003**(1999).

14. V. Tripathi *et al.*, Phys. Rev. Lett. **88**, 172701 (2002).

15. C. Beck *et al.*, Phys. Rev. C **67**, 054602 (2003).

16. A. Diaz-Torres and I. J. Thompson, and C. Beck, Phys. Rev. C **68**, 044607 (2003); arXiv:**nucl-th/0307021**(2003).

17. A. Diaz-Torres, I. J. Thompson, Phys. Rev. C **65**, 024606 (2002); arXiv: **nucl-th/0111051**(2001).

18. G. V. Marti *et al.*, Phys. Rev. C **71**, 027602 (2005).

19. C. Beck, A. Sànchez i Zafra, A. Diaz-Torres, I. J. Thompson, N. Keeley, and F. A. Souza, AIP Conferences Proceedings **853**, 384 (2006); Proc. of Fusion06 Conference, San Servolo, Venezia, Italy, 19-23 March 2006; arXiv: **0605029** [nucl-th] (2006).

20. C. Beck, N. Keeley and A. Diaz-Torres, Phys. Rev. C **75**, 054605 (2007); arXiv:**nucl-th/0703085** (2007).

21. C. Beck, Nucl. Phys. A **787**, 251 (2007); arXiv:**nucl-th/0610004** (2006).

22. C. Beck *et al.*, Nucl. Phys. A **834**, 440 (2010); arXiv: **0910.1672** [nucl-ex] (2009).

23. G. R. Kelly *et al.*, Phys. Rev. C **63**, 024601 (2000).

24. A. Pakou *et al.*, Phys. Rev. Lett. **90** 202701 (2003)

25. D.J. Hinde, M. Dasgupta, B. R. Fulton, C. R. Morton, R. J. Wooliscroft, A. C. Berriman, and K. Hagino, Phys. Rev. Lett. **87**, 272701 (2002).

26. A. Diaz-Torres, D. J. Hinde, J. A. Tostevin, M. Dasgupta, and L. R. Gasques, Phys. Rev. Lett. **98**, 152701 (2007); arXiv:**nucl-th/0703041**(2007).

27. Y. Tokimoto *et al.*, Phys. Rev. C **63**, 035801 (2001).

28. M. M. de Moura *et al.*, Nucl. Instr. Meth. A **471**, 368 (2001).

29. A. Shrivastava *et al.*, Phys. Rev. Lett. **103**, 232702 (2009).

30. G. G. Ohlsen, Nucl. Instr. Meth. **37**, 240 (1965).

31. D. Scholz *et al.*, Nucl. Phys. A **288**, 351 (1977).

32. J. E. Mason *et al.*, Phys. Rev. C **45**, 2870 (1992).

33. R. Kanungo *et al.*, Nucl. Phys. A **599**, 579 (1996).

34. K. Alder *et al.*, Rev. Mod. Phys. **28**, 432 (1956).

35. D.R. Tilley *et al.*, Nucl. Phys. A **708**, 3 (2002).

36. P.K. Rath *et al.*, Phys. Rev. C **79**, 051601 (2009).